J. Materials, Conc. Struct., Pavements, JSCE, No.669/V-50, 293-307, 2001 February

MULTI-DIRECTIONAL FIXED CRACK APPROACH FOR HIGHLY ANISOTROPIC SHEAR BEHAVIOR IN PRE-CRACKED RC MEMBERS

Amorn PIMANMAS[1] and Koichi MAEKAWA[2]

[1] Member of JSCE, Ph.D., Research fellow, Dept. of Civil Eng., The University of Tokyo
(Hongo 7-3-1, Bunkyo-ku, Tokyo 113, Japan)
[2] Member of JSCE, Dr. of Eng., Professor, Dept. of Civil Eng., The University of Tokyo
(Hongo 7-3-1, Bunkyo-ku, Tokyo 113, Japan)

Recent experiments on pre-cracked beam conducted by the authors pose challenge to the numerical analysis in the field of reinforced concrete mechanics. The numerical requirements of pre-cracked beam problem are identified as (1) multi-step loading paths and path-dependency transfer, (2) multidirectional cracks with crack interaction and (3) highly anisotropic shear along pre-crack plane. Four-way fixed crack approach is judged to fulfil the above numerical requirements. The finite element analysis of pre-cracked beam is conducted. It is verified that the four-way fixed crack approach can reliably reproduce the experimental results of pre-cracked beam

Key Words: *pre-cracked RC members, crack interaction, shear anisotropy, fixed crack approach Multi-step loading path*

1. INTRODUCTION

The influence of vertical pre-cracks on RC behaviors subjected to shear has been investigated in the experiments recently conducted by the authors[1]. Experimental results showed that vertical pre-cracks could greatly affect shear behavior of RC beam in terms of loading capacity, failure characteristics and load-displacement relation. When vertical pre-cracks exist, the loading capacity is greatly increased.

It was found that the width of pre-crack is the main factor that affects the failure behavior. Rationale in mechanics of pre-cracked element exists, which can explain all experimental results and associated phenomena. This mechanics rationale is based upon the shear anisotropy along pre-crack plane.

This paper aims at analytically investigating the behavior of pre-cracked members. The authors suppose that the rationale in mechanics is the core for the analytical simulation. However, the closed form solution may not be easily obtained in the structural or member level due to the complexities of the problem. In this paper, the finite element method is judged to suit the problem since the overall member behavior can be assembled from the element behavior. As a matter of fact, the rationale in mechanics can be reproduced in the finite element analysis based upon the local crack behavior.

The first part of this paper reviews the authors' recent experimental observations and findings. Before the numerical investigation, the numerical requirements of the pre-cracked beam problems are indicated. It will be argued that not all crack methods available in literature can solve the problem. The authors then briefly review available crack schemes and point out their limitations and applicability. Finally, it is judged that the multiple fixed crack approach may be most appropriate for the pre-cracked beam problem. Then the finite element analysis is conducted and the comparison with experiment is discussed.

2. SHEAR TEST OF PRE-CRACKED BEAMS: REVIEW OF THE AUTHORS' EXPERIMENT

Before proceeding to the numerical investigation, the brief review will be helpful for understanding the phenomena and the numerical requirements of the pre-cracked beam problem. Experimental outline is shown in **Fig.1**. The loading procedure was composed of two steps (**Fig.1**). The first step applied reversed flexural loading to introduce vertical pre-cracks penetrating the entire sections.

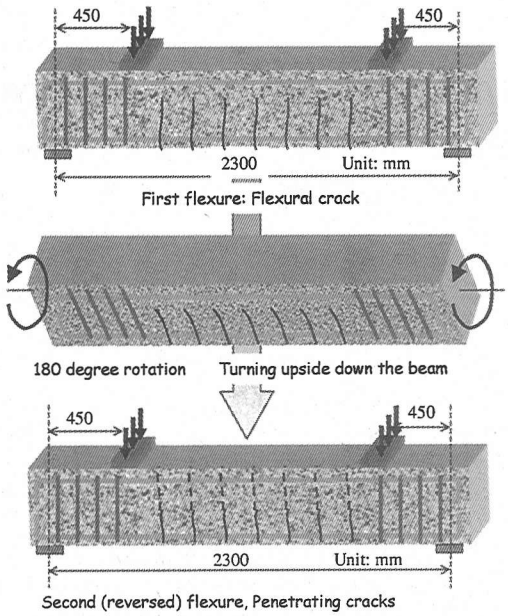

(a) First step reversed flexural loading

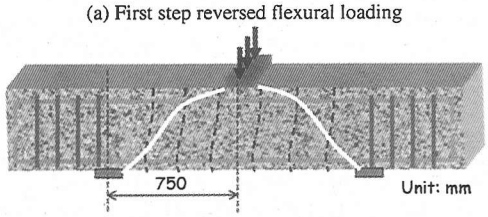

(b) Second step shear loading

Fig.1 Loading set up in the author's experiment

The second step applied shear loading to cause diagonal shear crack propagating across the vertical pre-crack planes. In order to induce shear crack, bearing supports were shifted towards beam mid-span such that the shear span to effective depth ratio was 2.41. Typical load-displacement relationship of pre-cracked beam is shown in **Fig.2** in comparison with the non pre-cracked beam. It is seen that pre-cracked beam shows considerably higher capacity, ductility, energy consumption but lower stiffness. Failure crack pattern of pre-cracked and non pre-cracked beams is compared in **Fig.3**. The failure of the non pre-cracked beam is due to the unstable propagation of a single diagonal crack (**Fig.3a**). On the contrary, the propagation of a diagonal crack in the pre-cracked beam is not continuos, but arrested by vertical pre-cracks. This results in the phenomenon of crack arrest and diversion[1], which explains the large increase in loading capacity.

The failure in pre-cracked beam is caused by the formation of several independent diagonal cracks that combine together into a single crack along the failure path. The behavior of pre-cracked beam can

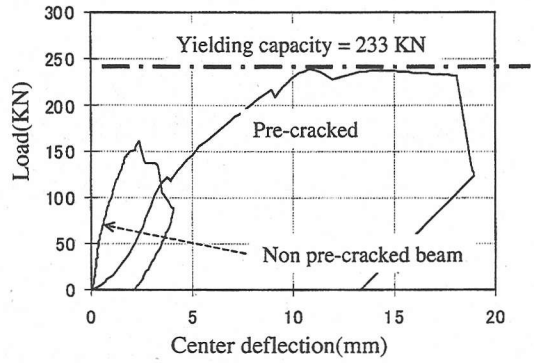

Fig.2 Typical load-displacement relation of pre-cracked beam

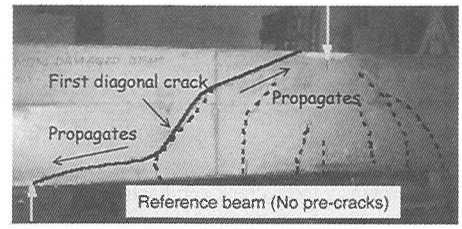

(a) Failure crack pattern of non pre-cracked beam

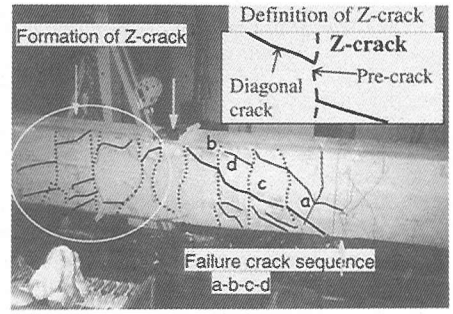

(b) Failure crack pattern of pre-cracked beam

Fig.3 Experimental Failure crack pattern

be explained in terms of the relative deformational behavior between pre-crack and diagonal crack or the crack interaction. Due to the mutual contribution of pre-crack and diagonal crack, the crack formed in pre-cracked beam has Z-shape pattern (referred to as Z-crack as shown in **Fig.3b**).

Pre-cracks affect not only post-diagonal crack behavior but also pre-diagonal crack behavior. The load-displacement of pre-cracked beam (**Fig.2**) shows initial non-linearity due to deformation of pre-cracks. All experimental observations can be explained by the shear anisotropy along pre-crack plane[1]. Due to the anisotropy and shear slip along pre-crack, principal stresses will not generally coincide with principal strains. The imposed total strain is mainly transformed into the slip along pre-crack, thus, the diagonal stress is relaxed. This explains the arrest of diagonal crack propagation at the pre-crack plane.

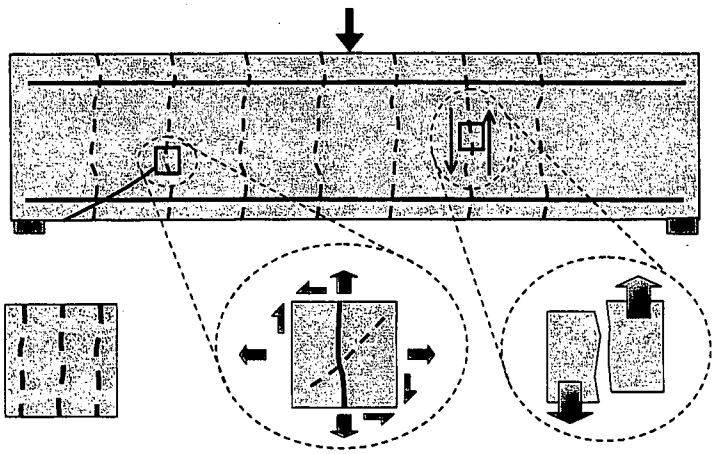

REQUIREMENT 1
Multi-step loading path,
Transfer of path dependency information

REQUIREMENT 2
Multi-directional cracks
Crack interaction
Relative deformation mode

REQUIREMENT 3
Anisotropy in shear
Shear slip and shear transfer
along pre-crack interface

Fig.4 Numerical requirements of the pre-cracked beam problem

3. NUMERICAL REQUIREMENTS OF THE PRE-CRACKED BEAM PROBLEM

Before performing the numerical investigation, the numerical requirements of the pre-cracked beam problems are pointed out as follows (**Fig.4**),

(1) Multi-step loading path and path-dependency transfer

In the experiment, two loading steps are employed. The first step is reversed flexural loading to introduce pre-cracks and the second step is shear loading to apply shear crack penetrating the pre-crack planes. It is noted that not only loading condition but also support configuration changes from the first to the second step. The loading pattern is described as non-proportional multi-step loading path.

In this case, the analysis cannot be carried out in a single step. The analysis needs to be divided into two sequential sub-steps with different loading and boundary conditions. Therefore, it is necessary that the pre-crack condition in the first step must be transferred to the second step as the initial condition. Not only pre-crack state, but also other state variables and nodal degree of freedom have to be properly managed. The state variables include state of stress/strain and cracking information at Gauss points. Nodal degree of freedom includes force and displacement. The first requirement of the analysis scheme is that it must be able to record and transfer path-dependency for the correct representation of material states.

(2) Multi-directional cracks with crack interaction

The crack pattern in the pre-cracked beam clearly shows that two systems of cracks co-exist, the pre-crack and diagonal crack. It is discussed that the behavior of pre-cracked beam is governed by the crack interaction or the mutual contribution of pre-crack and diagonal crack. Therefore, in the pre-cracked beam problem, the analysis scheme must be able to manage the multi-directional cracking situation. It must be able to detect which crack is to be active or dormant. In other words, the relative deformational behavior of each crack in the element or the crack interaction has to be handled properly by the analysis scheme. It is noted that the shear behavior of the non pre-cracked beam is less complicated since it involves only one crack system.

(3) Highly shear anisotropy along weak plane of pre-cracks.

The third requirement is the strong anisotropy along pre-crack plane[1]. Due to pre-crack, the element behavior cannot be defined as isotropic. Principal stresses will not generally coincide with principal strains. To take the shear anisotropy into account, the normal crack stress release and the shear transfer along the crack interface must be explicitly modeled in the analysis scheme. In other words, the shear behavior is no longer dependent on normal action, but must be directly related to the aggregate interlock along the crack interface.

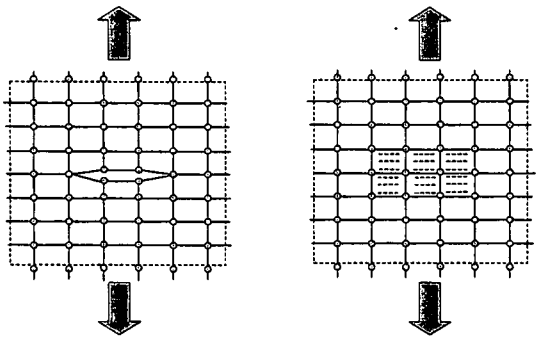

(a) Discrete concept (b) Smeared concept

Fig.5 Representation of crack in FEM

4. CRACK SCHEMES IN LITERACTURE

In the previous section, three numerical requirements of the pre-cracked beam problem have been identified. The authors will take a brief review of crack schemes available in literature and discuss the one that can fulfil the above numerical requirements.

(1) Discrete versus smeared crack approaches

In the finite element analysis, two main different disciplines for representing cracks exist. They are so-called *discrete crack approach* and *smeared* or *distributed crack approach.*

In discrete crack approach[2], cracks are idealized as the separation between two adjacent finite elements (**Fig.5a**). The interface elements are installed to represent discrete crack directly. For the problems in which the directions and locations of cracks cannot be specified in advance, the use of discrete crack approach may be inconvenient since new elements and nodes must be added for each formation of new crack. This results in the modification of finite element mesh and may require significant computational time and cost.

However, the use of discrete crack approach may be helpful for problems where locations of discontinuity can be clearly identified. These include interfaces at the interconnection of RC members with substantial difference in stiffness[3], interfaces between different material contacts such as structural steel/concrete, concrete/soil and reinforcement/concrete to model bond slip.

Another crack approach is the smeared crack method[4]. In this method, cracked concrete is considered as continuum with the same finite element mesh preserved throughout the analysis (**Fig.5b**). Cracking is modeled by changing the material stiffness appropriately. The smeared crack approach is relatively attractive for the problem in

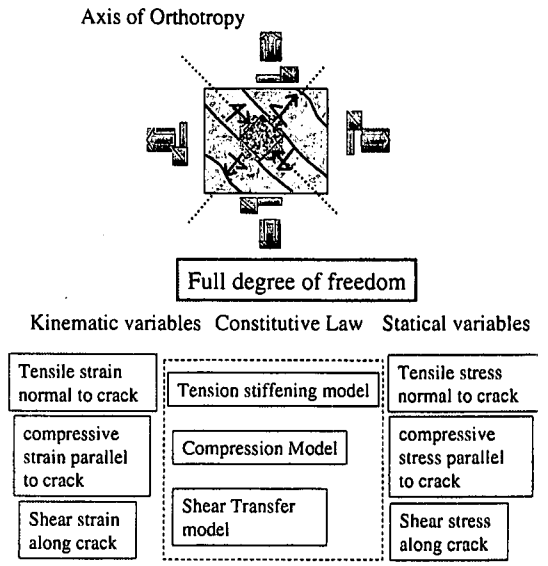

Fig.6 Full degree of freedom in fixed crack scheme

which the directions or locations of cracks are not known in advance[3].

(2) Classification of smeared crack approach

Fixed versus rotating crack scheme

a) Fixed crack approach

In the fixed crack approach[3),5)], crack is described to be fixed upon its generation. The main idea of the fixed crack approach is that it explicitly considers Mode I normal crack stress release and Mode II shear traction transfer. These two behaviors have their real physical backgrounds in terms of aggregate bridging and interlock, respectively. The importance of mode I normal traction is clear since it enables the objectivity regarding the mesh size for the application of fracture mechanics in finite element analysis.

However, the modeling of mode II shear transfer has not received much attention and the clear understanding of shear fracture energy is not available. The authors wish to point out that the mode II shear transfer is also crucial for the correct modeling of crack behavior. In the element level, the fixed crack approach considers maximum degree of freedom of the element. This allows the independent treatment of shear and normal actions (**Fig.6**), which is the basic requirement for the anisotropy.

In the 2-D context, kinematic variables include tensile strain normal to a crack, compressive strain parallel to a crack and shear strain along crack interface. Corresponding static variables include tensile stress normal to a crack, compressive stress parallel to a crack and shear stress along crack

interface. The relationships between kinematic and static variables are described by constitutive equations.

Another prominent character of the fixed crack approach is that the crack memory and path-dependency are permanently recorded unless the computation is finished. This enables the appropriate treatment of path-dependency as one of the numerical requirements.

b) Rotating crack approach

In the rotating crack approach[6),7),8),9)], it is assumed that the axis of orthotropy, i.e., axis along which stresses are computed, coincide with the principal strain direction. This implies that principal stress vector coincides with principal strain vector, which is known as the co-axiality principle. The co-axiality principle is essentially equivalent to the isotropy. Since shear stress vanishes on the continually updated principal planes where stresses are computed, the consideration of shear transfer is not needed. Only normal stress-strain relations in the direction normal and parallel to the crack axis are needed.

Due to the isotropy assumption, the rotating crack approach cannot treat shear slip and shear traction transfer due to aggregate interlock. Furthermore, in the rotating crack approach, only one crack is considered at one time, thus, the path-dependency needs not be recorded. Moreover, this also means that the multi-cracking condition and crack interaction cannot be taken into account. From this discussion, it is concluded that the rotating crack approach cannot fulfil any of the above numerical requirements and thus not applicable to the pre-cracked beam problem.

5. FOUR-WAY FIXED CRACK MODEL

From the above discussion, it is clarified that the fixed crack approach may be more appropriate for the pre-cracked beam problem. The fixed crack approach records all cracks and thus allows multi-cracks to be considered. The path dependency can be transferred among load steps. The crack interaction can be handled by the active crack concept[3)]. The shear anisotropy can be taken into account by the explicit and independent treatment of shear and normal stress transfer.

One of the recent developments in line with the fixed crack scheme is the multi-directional four-way fixed crack approach proposed by Fukuura and Maekawa[10),11)]. This crack scheme was installed in the WCOMD[3)] general nonlinear path-dependent finite element analysis program, which will be used for the numerical investigation in this paper.

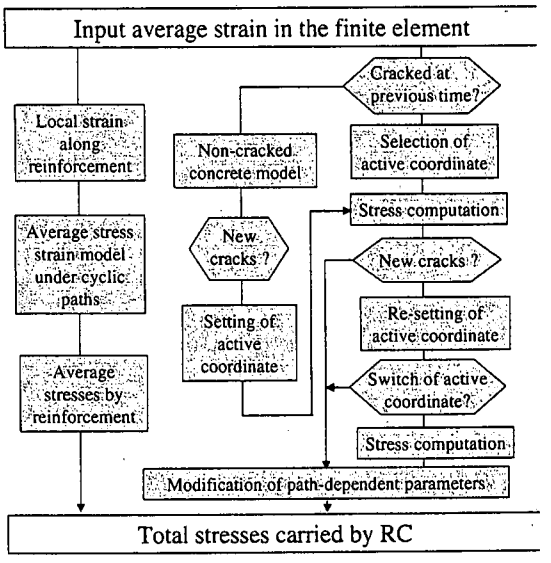

Fig.7 Computational scheme for 4-way fixed crack approach

Four-way fixed crack model can be regarded as the generalization of two-way cracking approach[3)], implemented such that up to four cracks in arbitrary orientations at any Gauss point can be covered. The active crack hypothesis is still preserved but the applicability has been extended to the co-ordinate level.

In the scheme of four-way cracking concept, a maximum of two orthogonal co-ordinates can be established at the integration point of the element. In each co-ordinate, at most 2 cracks are allowed. Two cracks associated with a co-ordinate system need not be perfectly orthogonal but must satisfy the quasi-orthogonal condition that the angle between them is larger than 67.5° but less than 112.5°. Upon the generation of the first crack, the first co-ordinate system is established. If the next crack is generated and meets the aforementioned angular criterion, it will be treated in the same co-ordinate, otherwise, the second co-ordinate is set-up. The assignments of the co-ordinate systems and the generation of new cracks will be implemented according to this rule until up to four-way cracks have been induced into the Gauss point of RC element.

Fig.7 describes the flow of stress computation in this scheme. The active crack concept is based on the fact that under the multi-cracking condition, overall non-linearity is generally prevailed by certain cracks while others are hardly activated. The crack of which normal strain is smaller is considered dormant due to its relatively higher stiffness. In each co-ordinate, the stress computation will be undertaken along the selected active crack. Then the active co-ordinate will be judged by comparing the normal strain of the active crack in each co-ordinate. Ultimately, the final stress output of the

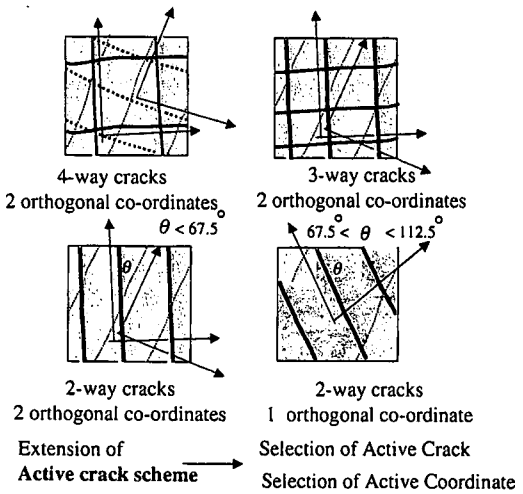

Fig.8 Coverage of four-way fixed crack approach[10),11)]

element will be entirely governed by the crack in the selected active co-ordinate. Regarding revision of path-dependent parameters, since the concrete stresses along normal and parallel to cracks are highly-path dependent, the update of path-dependent parameters is carried out in both active and dormant co-ordinates. However, the evolution of shear is hardly mobilized in the dormant co-ordinate, thus shear related path dependency is not revised in the step computation.

Fig.8 shows the coverage of four-way fixed crack approach applied to RC smeared elements with 2, 3 and up to four-way cracks in arbitrary directions. In general, any number of cracks can be covered by adding more orthogonal co-ordinate systems and refining the criterion for introducing these co-ordinates. However, such implementation is hardly justified since it may be quite rare to encounter cracked elements of more than four independent directions. Moreover, adding more co-ordinates not only complicates the analysis but also requires more computational time for recording path-dependent parameters and stress computation process. The authors judge that four-way fixed crack approach is sufficient for dealing with cracked reinforced concrete in most engineering situations.

6. LOCAL CONSTITUTIVE MODELS

In line with the fixed crack approach, the local constitutive laws are formulated along the crack axis. The global imposed strain vector of a RC element is transformed into local strains along the crack and reinforcement directions by the transformation rule. Then, local constitutive laws are applied to compute local stresses from decomposed local strains for both concrete and reinforcing bars. Once again, through the transformation rule, these local stresses will be transformed back to the global system. Through compatibility, total stress vector of a RC element in the global co-ordinate is obtained from the direct superposition of concrete and reinforcement stress vectors.

(1) Concrete[10),11)]

The local strain vector of concrete consists of strain normal to a crack, ε_n, strain parallel to a crack, ε_t, and the shear strain along crack interface, γ_{cr}. Input variables for local constitutive laws are local strains defined above as well as necessary path-dependent parameters. The local constitutive laws are formulated for both envelope and internal loops. The constitutive laws can be defined as the uni-axial relations between the average stress and average strain as follows,

$$\sigma_n = \sigma(\varepsilon_n, \varepsilon_t, \eta_{1,2,\ldots,n}) \quad (1)$$

$$\sigma_t = \sigma(\varepsilon_t, \varepsilon_n, \eta_{n+1,\ldots,2n}) \quad (2)$$

$$\tau_c = \tau(\gamma_{cr}, \varepsilon_n, \varepsilon_t, \eta_{2n+1,\ldots}) \quad (3)$$

where σ and τ represent the constitutive laws for computing normal and shear stresses, respectively. η represents the set of path-dependent parameters for memorizing the loading path. The formulation of the above constitutive laws and the path-dependent parameters are already reported[10),11)]. In the following, only the formula for envelope will be given.

The above constitutive laws correspond to three degree of freedom of a cracked element, namely, tension stiffening/softening model normal to the crack, compression model parallel to the crack and shear transfer model along the crack interface. The coupling between shear and normal action is not explicitly considered in the formulation of stiffness matrix. The shear dilatancy is implicitly considered by adding the induced compressive normal stress due to shear to the computed normal stress orthogonal to the crack axis.

a) Coupled compression-tension model for normal stresses parallel and perpendicular to crack

The constitutive law for computing normal stresses (denoted as σ in Eq.1 and Eq.2) is the coupled compression-tension model as shown in **Fig.9**. For concrete in tension, the model covers both the softening due to aggregate bridging at the crack plane as well as the tension stiffening effect due to bond stress transfer between concrete and steel bar. For envelope in tension, the model can be expressed as,

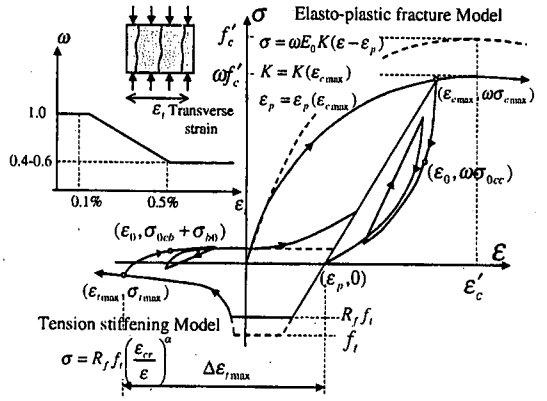

Fig.9 Coupled compression-tension model for normal stresses parallel and perpendicular to crack[10), 11)]

$$\sigma = \sigma_n = f_t \left(\frac{\varepsilon_{tu}}{\varepsilon_n} \right)^c \tag{4}$$

where σ is the tensile stress transfer normal to crack, ε_{tu} is the cracking strain, c is softening/stiffening parameter[10),11)].

For compression parallel to the crack direction, the normal stress is computed from the continuum deformation. For envelope, the elasto-plastic fracture model[3)] is used,

$$\sigma = \sigma_t = K_0 E_{c0} (\varepsilon_t - \varepsilon_p) \tag{5}$$

where K_0 is the fracture parameter, E_{c0} is the initial stiffness and ε_p is the compressive plastic strain. The model combines the non-linearity of plasticity and fracturing damages to account for the permanent deformation and loss of elastic strain energy capacity, respectively. The reduced compressive stress transfer ability due to transverse tensile strain[3)] is considered as additional damage[12)] by factorizing the normal coupled stresses by ω as,

$$\sigma_t = \sigma(\varepsilon_t, \varepsilon_n, \eta_{n+1,\ldots,2n}) = \omega(\varepsilon_n) \cdot \sigma(\varepsilon_t, \eta_{n+1,\ldots,2n}) \tag{6}$$

b) Shear transfer model

For computing shear stress transfer along the crack interface and the shear stiffness of the crack, the contact density model[13)] is used for the envelope. Thus, Eq. 3 can be expressed as,

$$\tau = f_{st} \frac{\beta^2}{1+\beta^2} \tag{7}$$

$$G_{cr} = \frac{\tau(\beta)}{\gamma_{cr}} \tag{8}$$

where f_{st} is shear strength transfer along the crack.

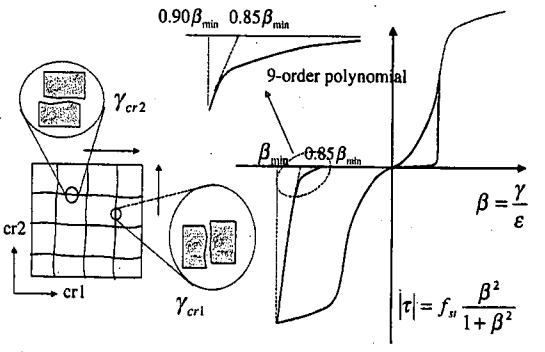

Fig.10 Shear transfer model[10), 11)]

β is the normalized shear strain defined as follows,

$$\beta = \frac{\gamma_{cr}}{\varepsilon_n} \tag{9}$$

For the cracked RC element, The imposed total shear strain (γ) compatible with the assumed nodal displacement can be separated into the shear strain due to un-cracked concrete part (γ_0) and shear strain due to cracks (γ_{cr}) as,

$$\gamma = \gamma_0 + \gamma_{cr} \cong \gamma_{cr} \tag{10}$$

Generally, shear strain due to un-cracked concrete part is relatively small compared with crack shear strain, thus it can be ignored. For the active co-ordinate, which contains two-way cracks, the crack shear strain must be decomposed into the shear strain along each crack as,

$$\gamma_{cr} = \gamma_{cr1} + \gamma_{cr2} \tag{11}$$

γ_{cr1} and γ_{cr2} denote the local shear strain along each crack which will be input to the shear constitutive law to compute shear stress transfer along each crack, respectively.

Since each crack can be independently subjected to loading, unloading or reloading conditions. The component of shear strain along each crack direction must be determined such that the equilibrium of shear stress is satisfied as (**Fig.10**),

$$G_{cr1}(\gamma_{cr1}, \varepsilon_{n1}, \eta_1) \cdot \gamma_{cr1} = G_{cr2}(\gamma_{cr2}, \varepsilon_{n2}, \eta_2) \cdot \gamma_{cr2} \tag{12}$$

The overall shear modulus of the element (G) considering two-cracks can be expressed as;

$$G = \frac{1}{\frac{1}{G_c} + \frac{1}{G_{cr1}(\gamma_{cr1}, \varepsilon_{n1}, \eta_1)} + \frac{1}{G_{cr2}(\gamma_{cr2}, \varepsilon_{n2}, \eta_2)}} \tag{13}$$

where G_c is the secant shear modulus of un-cracked concrete and G_{cri} is the secant shear modulus of the i-th crack.

(2) Modeling of reinforcing bar

Local strain vector of reinforcing bar is defined along the bar axis. Reinforcing bar is modeled in the smeared concept, that is, it is assumed uniformly distributed over the whole element. This representation is more advantageous than discrete one since no additional nodes and elements are required.

For reinforcing steel bar, compressive strains are usually smaller than tensile strains, thus preventing reinforcement from excessive yielding in compression before spalling of concrete cover has occurred. At the tension side, however, the highly localized plasticity at the vicinity of cracks has to be taken into account. It is known that bond transfer between concrete and steel has to be considered in the average stress-average strain relations of both concrete and reinforcement. For concrete, this is known as tension stiffening effect[3]. For reinforcing bar, it is shown that, due to bond effect, average yield stress is reduced compared with bare bar[3]

Thus the modeling of reinforcing bar in compression and tension can be different. For compression, the bilinear bare bar model is assumed in the analysis. For tension, the average stress-strain relationship considering the effect of localized plasticity as originally proposed by Okamura and Maekawa[3], and further refined by Salem and Maekawa[14] in consideration of very high plastic strain, is adopted. **Fig. 11** shows modeling of reinforcing bars for both envelope and internal loops representing path-dependency treatment[10),11)]

Since cracks in reinforced concrete element need not be orthogonal with the reinforcement direction, the bond effect cannot be expected fully functional in such case. Reinforcing bar orthogonal to crack is supposed to have full bond effect. On the contrary, reinforcing bar parallel to crack is supposed to follow bare bar behavior. Therefore, the computation of mean yield strength has to take into account the angular deviation of normal to crack from reinforcing bar direction[10),11)] (**Fig.11**).

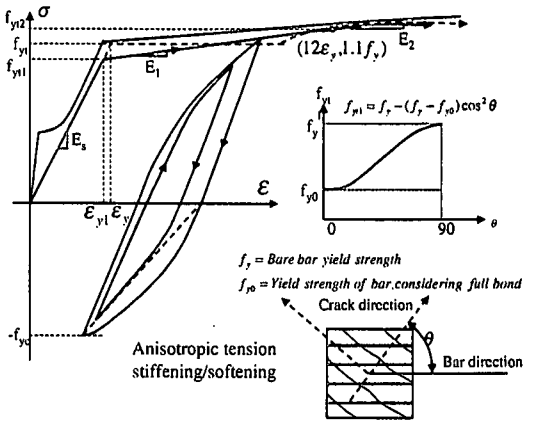

Fig. 11 Modeling of reinforcing bar[10),11)]

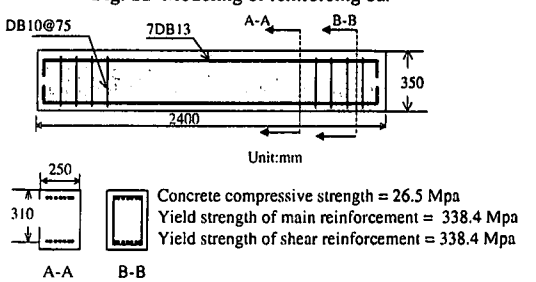

(a) Dimension of specimen and material properties

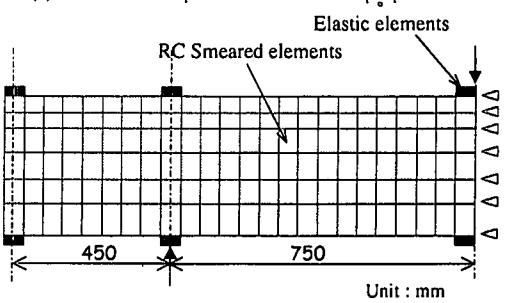

(b) Finite element mesh

Fig.12 Specimen dimension, material properties and finite element mesh

7. NUMERICAL VERIFICATION

In this section, the experiment conducted by the authors[1)] will be simulated. Three beams will be analyzed. Beam 1 is the reference beam without pre-cracks. Beam 2 and 3 represent pre-cracked beams. The level of reversed flexural loading assigned to these beams is different in order to introduce pre-cracks with different width into them. The width of pre-crack in beam 2 is given much larger than in beam 3. In the experiment, crack pattern and failure behavior were different between beam 2 and beam 3. The capability of four-way fixed crack approach in capturing the effect of crack width will be checked.

Specimen dimension, cross section, reinforcement arrangement and material properties are shown in **Fig.12a**. The reinforcement ratio of main bar is 1.14 %. Tested concrete compressive strength is 26.5 Mpa. Tested yield strength of main bar is 338.4 Mpa. The same finite element mesh used for these three beams is shown in **Fig.12b**. Due to symmetry, the analysis of half-beam is sufficient for saving computational time. Elastic elements are provided at the loading point and support to gradually distribute

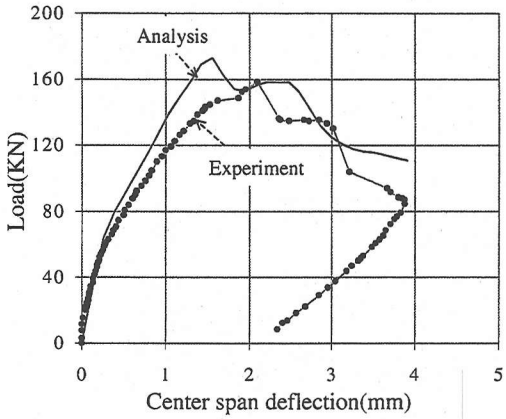

Fig.13 Load-displacement relation of non pre-cracked beam

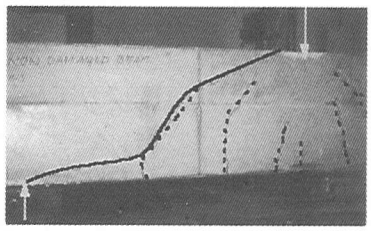

(a) Experimental[1)]

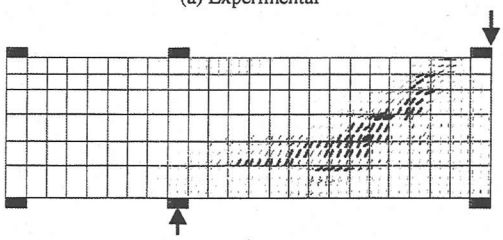

(b) Numerical

Fig.14 Failure crack pattern of non pre-cracked beam

the applied load over a sufficient area into the main body of the beam. Without them, the localized stress concentration due to direct point contact between load and RC elements can lead to premature failure. In the experiment, steel bearing plates were actually provided for this purpose. The numerical load application is implemented through the step increment of forced displacement at the specified node.

(1) Analysis of beam 1: reference case

Beam 1 is the non pre-cracked beam. Since, the behavior is governed by diagonal crack only, the analysis does not check the capability of multi-direction crack scheme. However, the capability of WCOMD in capturing the localization can be directly scrutinized. In this case, the multi-directional crack scheme must capture the dominant role of diagonal crack as one extreme of the crack scheme.

WCOMD currently incorporates the treatment of fracture mechanics through a zoning concept proposed by An and Maekawa[15)]. In this approach, response of concrete fracture depends on its location relative to steel bars. Tension softening stress release model is assigned to concrete in the web zone, which is far from reinforcement, i.e., plain concrete zone (PL zone). On the other hand, tension stiffening model rooted in the interface bond between concrete and steel bar is assigned to RC elements near reinforcing bars, i.e., reinforced concrete zone (RC zone).

Numerical and experimental load-displacement relationships are compared in **Fig.13**. Fair agreement can be noticed. Analysis slightly overestimates loading capacity and stiffness. Prediction of post-peak softening is currently possible but not accurate. It is noted that the softening behavior depends on the coupled deformation of cracks in mode I and mode II. Currently, the correct shear softening model is not available. More research in this area is needed.

Numerical and experimental failure crack patterns are also shown in **Fig.14**. Analysis can predict the localization around the web zone of shear span similar to the experiment. This verifies that the FEM can successfully predict behavior of beam in which diagonal crack totally dominates, which represents one extreme where no pre-crack exists.

(2) Analysis of beam 2: beam containing large pre-crack

Next, the authors discuss the analysis of beam 2[1)]. Similar to the experiment, the analysis is composed of two steps. The first step applies reversed flexural loading for inducing pre-cracks. The second step applies shear loading to the beam. Numerical and experimental results representing the first step loading are shown in **Fig.15**. Close agreement can be obtained in terms of capacity, stiffness, residual deformation for both loading and unloading paths.

Initial pre-crack pattern resulted from this reversed flexure is illustrated in **Fig.16**. It is noted that localization of vertical pre-cracks (discrete cracks) can be captured despite the fact that only smeared elements are employed and constant bending moment is applied in the flexural span. In the figure, smaller width of pre-cracks is computed at the top fiber since it is subjected to compression in the reversed flexural loading. However the discrete localization captured in the analysis is not so perfect as in the experimental observation.

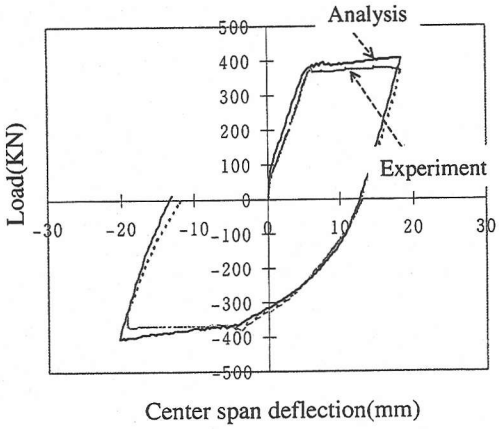

Fig.15 First step reversed flexure of beam 2: large pre-crack case

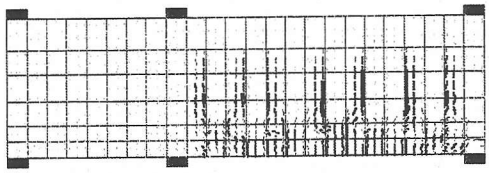

Fig.16 Numerical crack pattern after reversed flexure : beam 2: larger pre-crack case

The artificial discrete zones simulated by smeared element appear distributed in a larger band within the element size compared with real discrete cracks in the experiment. Furthermore, it is noted that cracks in RC elements in the tensile zone are more uniformly distributed over the element and over the flexure span. This implies that the localization prediction in the web zone (PL zone) is, to some degree, due to the mode I softening stress release implemented in the FEM for handling fracture mechanics. Nevertheless, such softening treatment does not ensure smeared scheme to perfectly reproduce discrete cracks.

In the second loading step, shear force is applied to the beam by means of three-point loading. In the experiment, bearing supports were moved towards mid-span such that the shear span to effective depth ratio was 2.41. In the analysis, this is implemented by changing the boundary condition of the problem. The fixed crack approach allows the transfer of pre-crack state and other state variables from reversed flexural loading to be the initial condition of the second stage shear loading. In the second analysis, shear is applied to the beam containing vertical pre-cracks. Initial loading stage successfully predicts Z-crack formation around each pre-crack similar to the experiment as shown in **Fig.17**.

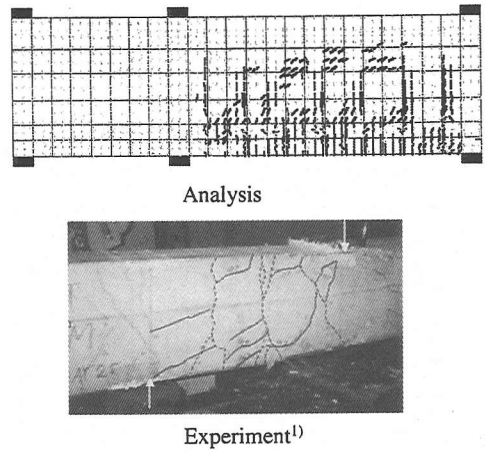

Fig.17 Z-crack in beam 2 : larger pre-crack case

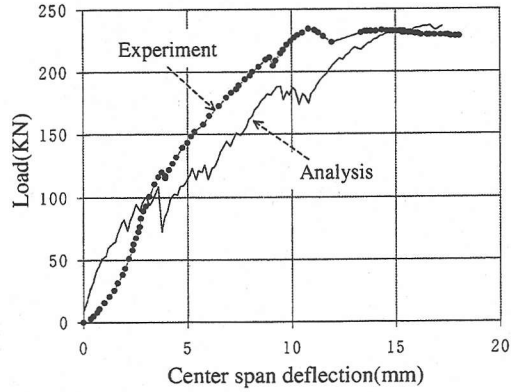

Fig.18 Comparison of load-displacement relations in beam 2: Experiment vs. analysis

Comparison between numerical and experimental results is shown in **Fig.18**. The ultimate capacity can be captured in the analysis. As can be observed from the figure, numerical load-displacement curve does not smoothly progress but shows the serrated pattern instead. In fact, experimental observation also demonstrated this behavior which is due to the crack arrest and diversion phenomenon. Once a diagonal crack is formed, load drops. However, since diagonal crack cannot propagate continuously at the pre-crack plane, further load can be resisted. This explains periodic cycles of temporary drop and increase in load-displacement curve, which are captured in both analysis and experiment. However the analysis seems to predict higher irregularity than the experiment. This is possibly due to the deficiency of smeared element in simulating discrete crack. Since the softening path is not recorded in the experiment, the analysis is conducted until the experimental failure point.

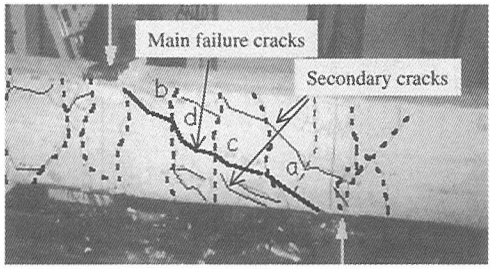

Experimental crack pattern[1)]

Secondary cracks captured by FEM

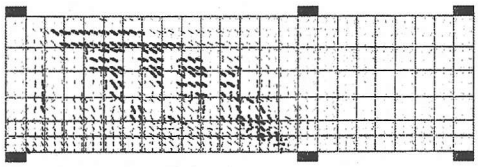

Main failure cracks captured by FEM

Fig.19 Failure crack pattern: smeared elements only

Final failure crack pattern is illustrated in **Fig.19**. In order to aid the visualization, two crack patterns corresponding to secondary and main failure cracks are separately drawn. Secondary cracks refer to those cracks that are located far from the web portion. Owing to their geometrical and positional attributes, the path of secondary cracks does not directly connect the loading point to support and hence hardly causes the ultimate failure. On the other hand, main failure cracks traverse the web region and directly link the loading point to support, enabling the successful formation of failure path. FEM can capture both crack paths consistently.

As shown in the failure crack pattern, the disconnected format of the main failure crack implies the successful reproduction of the independent formation of several discontinuous diagonal cracks. This also further means than the sequence in failure process can be correctly computed. In the pre-cracked beam, the ultimate failure is caused by the combination of several independent discontinuous diagonal cracks rather than the propagation of a single crack as in the non pre-cracked beam[1)].

Moreover, as clearly seen in **Fig.20**, no initiation of a new diagonal crack in a pre-cracked element is computationally predicted, which verifies the

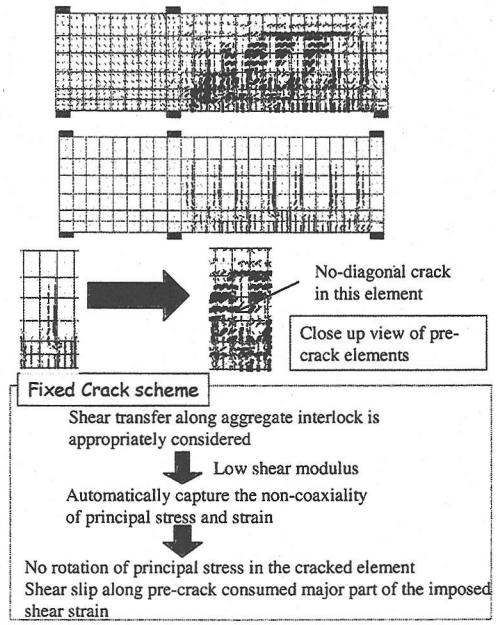

Fig.20 Initiation of diagonal crack in a pre-cracked element

significance of shear transfer. As stated, low shear transfer along pre-crack plane does not permit the rebuild of enough stresses for further cracking. This results in the crack arrest and diversion phenomenon and the discontinuity of diagonal cracks. The analysis verifies that shear anisotropy and crack interaction can be numerically predicted.

From the analysis results, it is seen that all essential characteristics of pre-crack elements and its effect on the structural member level can be captured well qualitatively and quantitatively. However, it is also judged that the smeared crack approach may not be perfect in simulating discrete cracks.

Therefore, it is instructive to undertake a comparative analysis in which pre-cracks are simulated by discrete joint elements[16)]. The propagation of diagonal crack, on the other hand, must be simulated by smeared elements in line with the fixed crack approach. Through the use of discrete joint elements, the authors suppose that the pre-cracks may be more properly represented. The generation and propagation of diagonal cracks should be the duty of FEM in selecting the most suitable failure path requiring minimum energy consumption.

Finite element mesh is shown in **Fig.21**. The loading step applied to the beam is the same as in the previous case in which only smeared elements are used. In the first step reversed flexural loading, the analysis agrees well with the experiment as

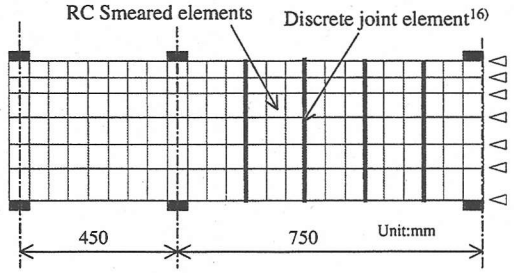

Fig.21 FEM mesh (half beam) for beam 2 using both smeared and discrete joint elements

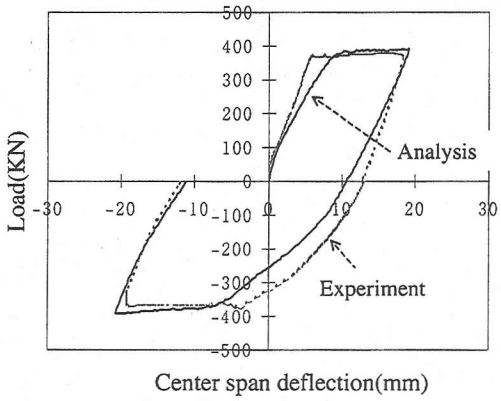

Fig.22 Load-displacement relationship under reversed flexure

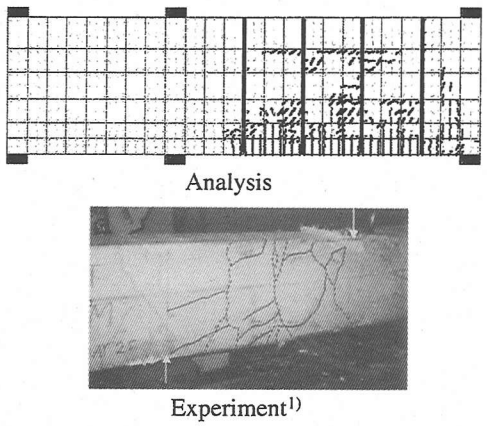

Fig.23 Initial crack pattern: capture of Z-crack formation

shown in **Fig.22**. Initial stage of shear loading exhibits Z-crack pattern similar to the experiment as shown in **Fig.23**. Both secondary and main failure crack patterns can be reproduced as shown in **Fig.24**. From the shape and position of numerical crack pattern, it is seen that the combined usage of both discrete joint and smeared elements gives better prediction to the experimental results than the use of smeared elements only. When only smeared

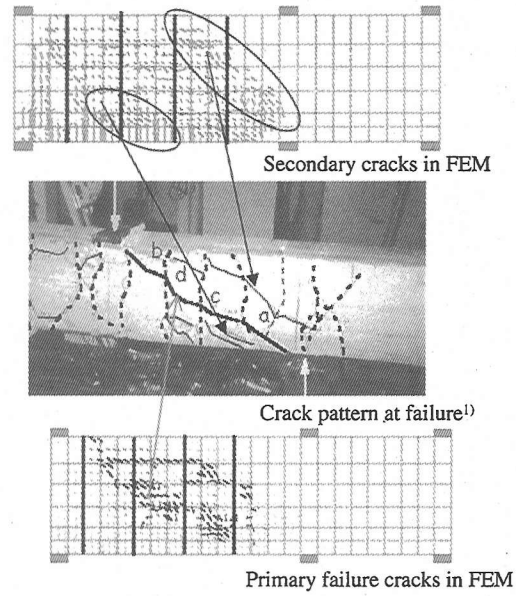

Fig.24 Failure crack pattern (beam 2, smeared + discrete joint)

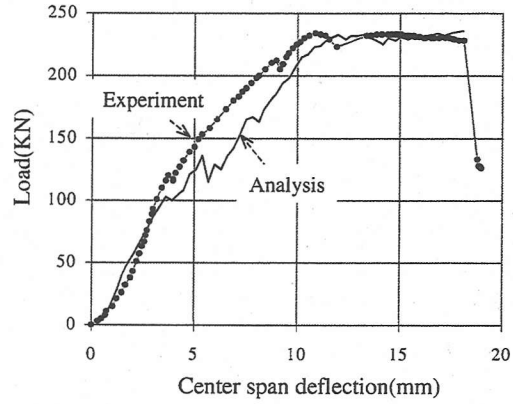

Fig.25 Comparison of load-displacement relations in beam 2 (smeared + discrete joints) : experiment vs. analysis

elements are used, main failure cracks are seen disjointed by the width of one element as shown in **Fig.19**. However, when discrete joint elements are used, the width of discontinuity band is significantly reduced (**Fig.24**). Load-displacement relationship is also well simulated with less irregularity as shown in **Fig.25**.

(3) Analysis of beam 3: Beam containing small pre-crack

In contrast to beam 2 in the previous analysis, beam 3[1)] contains smaller pre-cracks due to lower level of reversed flexural loading. Due to smaller pre-crack width, the Z-crack in the experiment has

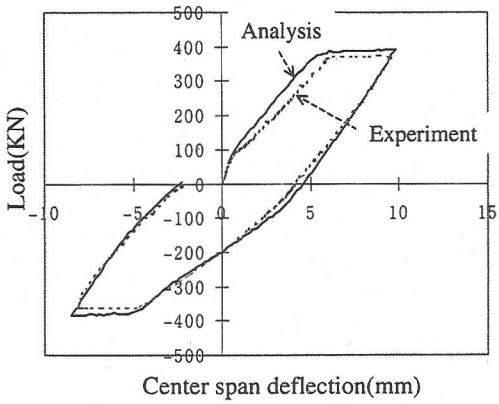

Fig.26 Load-displacement relationship of beam 3 (smeared only) under reversed flexural loading

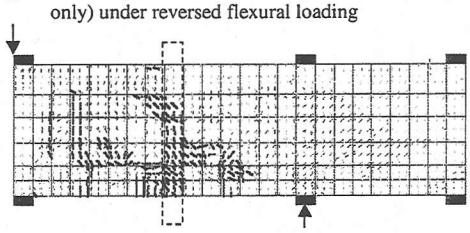

Numerical initial crack pattern: capture of Z-crack

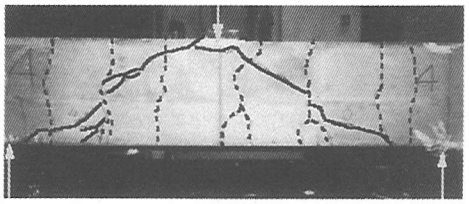

Experimental crack pattern[1)]

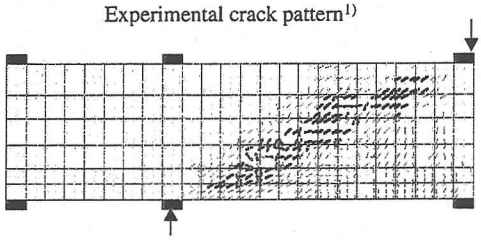

Numerical failure crack pattern

Fig.27 Crack pattern of beam 3(smeared only) : experiment vs. analysis

different shape from beam 2. The capability of FEM to reproduce the beam behavior when initial pre-crack is smaller will be investigated herein.

Similar to the foregoing analysis, two cases will be considered for beam 3[1)]. The first case uses only smeared elements while the second case uses both smeared and discrete joint elements. Unlike beam 2, the experimental initial crack pattern resulted from reversed flexural loading of beam 3 showed only one or two larger cracks in each side of the beam.

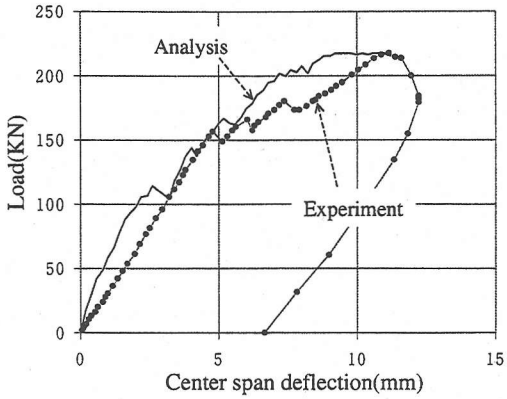

Fig.28 Comparison of load-displacement relations in beam 3 (smeared only) : experiment vs. analysis

The cracking extent is not uniform throughout the shear span. Therefore, in order to closely reproduce this initial pre-crack condition, only smeared or discrete joint elements, depending on the case, at the center of shear span are assigned lower tensile strength. The analysis in which only smeared elements are used is performed first. The first step reversed flexural loading shows good agreement between numerical and experimental results as shown in **Fig.26**. The transfer of path-dependency to the second analysis is the same as in the previous analysis. Initial stage of the second shear loading exhibits Z-crack mainly developed around the center portion of the shear span as shown in **Fig.27**. The geometry of this Z-crack fairly resembles the experimental result.

It is noted that the initial Z-crack pattern of beam 3 is quite different from beam 2. This reflects the difference in width of pre-crack and relative deformational contribution between pre-crack and diagonal crack[1)]. In the case of beam 2, several large pre-cracks are created owing to higher level of reversed flexure. This therefore results in several Z-cracks in which larger part is occupied by pre-crack and the constituent diagonal cracks are more distant apart. Finite element analysis conducted in the previous section succeeded in predicting the behavior of the beam containing large pre-cracks.

For the beam with smaller pre-cracks, FEM can also simulate Z-crack pattern in which diagonal crack is dominant. Therefore, the capability of FEM in reproducing the influence of the width of pre-crack is verified. Comparison of numerical and experimental load-displacement relationships is shown in **Fig.28**. Similar to beam 2, the softening path is not recorded in the experiment, thus the analysis is conducted until the experimental failure point.

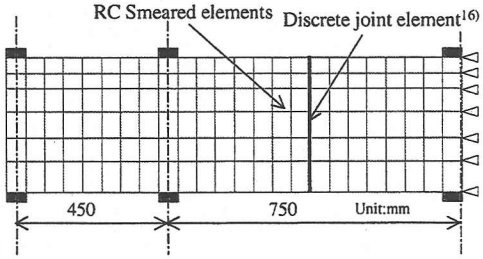

Fig.29 FEM mesh for beam 3 using both smeared and discrete joint elements

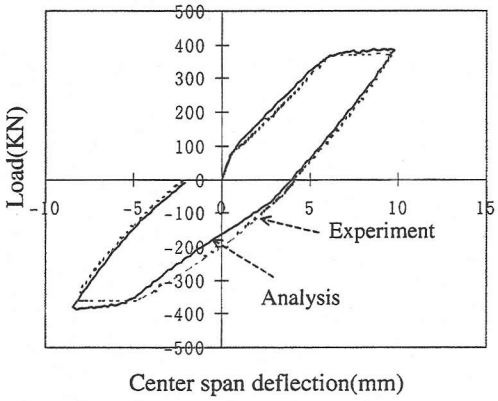

Fig.30 Load-displacement relationship of beam 3 (smeared + discrete joint elements) under reversed flexural loading

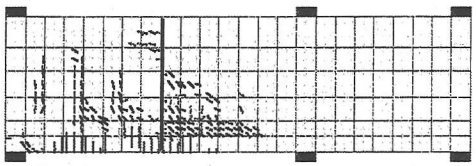

Numerical initial crack pattern: capture of Z-crack

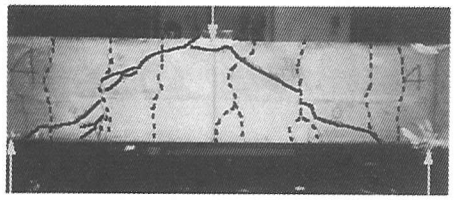

Experimental crack pattern[1)]

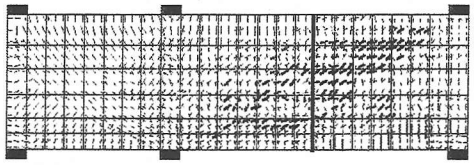

Numerical failure crack pattern

Fig.31 Crack pattern of beam 3 (smeared + discrete joint element): analysis vs. experiment

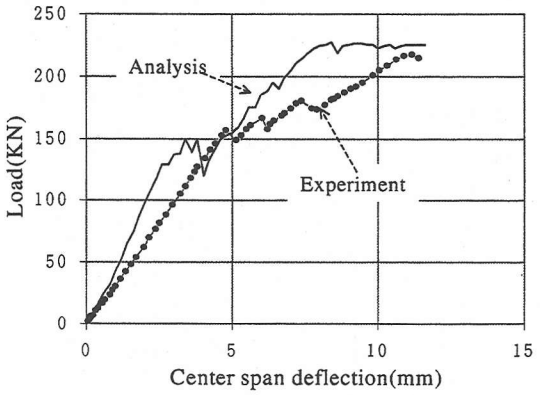

Fig.32 Comparison of load-displacement relations in beam 3 (smeared + discrete joints) : experiment vs. analysis

FEM can capture capacity well but it seems to predict higher stiffness. Typical erratic pattern noticed in the load-displacement curve due to discontinuity in the diagonal crack propagation can also be numerically computed. However reliable computation of displacement cannot be achieved in this analysis. Analytical failure crack pattern shows wider band of smeared cracks directly connecting loading point to support.

The second case employs one row of discrete joint elements at the center of shear span as shown in **Fig.29**. Even if experimental crack pattern shows several pre-cracks (**Fig.27**), but only pre-crack at the center of shear span is much larger than other cracks. Moreover, the experimental failure crack pattern shows Z-crack forming around the central pre-crack only (**Fig.27**). This verifies that the central pre-crack with larger width mainly arrests the crack propagation. Moreover, at the location where discrete joint elements are not installed in the mesh, the smeared element is shown to reproduce localization of pre-crack (**Fig. 16**). Therefore, the arrangement of discrete joint elements at the center of shear span of the beam only would be sufficient.

The analytical prediction is fundamentally similar to the case in which only smeared elements are used. Reversed flexural load-displacement relationship is shown in **Fig.30**. Initial and final failure crack patterns are shown in **Fig.31** for both experimental and numerical results. Z-crack can be captured. Numerical initial crack pattern in **Fig.31 (top)** also shows localization of vertical pre-cracks captured by smeared element. Load-displacement behavior under shear loading still exhibits higher stiffness as shown in **Fig.32**. But the first drop in load-displacement curve signifying the arrival of the first diagonal crack seems closer to the experimental result than the previous case. Failure crack pattern

as shown in **Fig.31** is similar to the previous prediction.

8. CONCLUSIONS

A numerical investigation of the pre-cracked reinforced members is conducted in this paper. Numerical requirements of the pre-cracked beam problem are identified, which include (1) multi-step loading path and path-dependency transfer, (2) multi-directional cracks with crack interaction and (3) highly shear anisotropy along pre-crack plane. It is judged that the four-way fixed crack approach can satisfy these numerical requirements and thus selected as the numerical tool.

In the fixed crack methodology, pre-crack condition and other state variables representing the environmental/loading history of RC members can be recorded and transferred over loading stages. Moreover, through the active crack concept, the multi-directional cracking situation with mutual interaction can be accounted for. Finally, the explicit treatment of mode I softening bridging and mode II aggregate interlock allows the independence of principal stress and strain vectors. Hence, shear anisotropy along the pre-crack plane is intrinsically taken into account. It may be concluded that the fixed crack approach models the crack behavior closest to the reality.

The numerical analysis verifies the validity of the four-way fixed crack approach in simulating the pre-cracked beam problem. The rationale in mechanics of pre-cracked element can be numerically reproduced with reasonable accuracy. Experimental behavior can be reliably predicted qualitatively and quantitatively. The influence of the width of pre-crack can be consistently analyzed, which verifies the significance of shear slip and the associated shear transfer along the crack interface.

ACKNOWLEDGEMENT: The authors express their gratitude to TEPCO foundation in providing financial supports for carrying out the experiment.

REFERENCES

1) Pimanmas, A., and Maekawa, K.: Influence of pre-crack on RC behavior in shear, Accepted for publication in J.Mater. Conc.struct. Pavements., *Proc. of JSCE*, 2001.
2) Ngo, D., Scordelis, A.C.: Finite element analysis of reinforced concrete beams, *J. Amer. Conc. Inst.*, Vol. 64(14), pp.152-163, 1967.
3) Okamura, H., and Maekawa, K.: *Nonlinear analysis and constitutive models of reinforced concrete*, Gihodo-Shuppan Co. Tokyo, 1991.
4) Rashid, Y.R.: Analysis of prestressed concrete pressure vessels, *Nucl. Eng. Design.*, Vol. 7(4), pp.334-344, 1968.
5) De Borst, R., and Nauta, P.: Non-orthogonal cracks in a smeared finite element model, *Eng. Comp.*, Vol. 2, pp. 35-46, 1985.
6) Cope, R.J., Rao, P.V., Clark, L.A., and Norris, P. : Modeling of reinforced concrete behavior for finite element analysis of bridge slabs, *Numerical Method for Nonlinear Problems 1*, Taylor C. et.al.(eds), Pineridge Press, Swansea, pp. 457-470, 1980.
7) Vecchio, F. and Collins, M.P. : The modified compression field theory for reinforced concrete elements subjected to shear, *ACI Journal*, Vol.3(4), pp. 219-231, 1986.
8) Vecchio, F.J.: Analysis of shear critical reinforced concrete beams, *ACI struct. J.*, Vol.97(1), pp.102-110, 2000.
9) Hsu, T.T.C.: ACI shear and torsion provisions for prestressed hollow girders, *ACI Struct. J.*,Vol. 94(6), pp.787-799, 1997.
10) Fukuura, N., and Maekawa, K.: Re-formulation of spatially averaged RC constitutive model with quasi-orthogonal bi-directional cracking, *Proc. of JSCE*, Vol. 45, pp. 157-176, 1999 (in Japanese).
11) Fukuura, N., and Maekawa, K.: Spatially averaged constitutive law for RC in-plane elements with non-orthogonal cracking as far as 4-way directions, *Proceeding of JSCE*, Vol.45, pp. 177-195, 1999 (in Japanese).
12) Miyahara, T., Kawakami, T., and Maekawa, K.: Nonlinear behavior of cracked concrete plate element under uniaxial compression, *Concrete Library International*, JSCE, Vol. 11, pp.306-319, 1988.
13) Li, B., Maekawa, K., and Okamura, H.: Contact density model for stress transfer across cracks in concrete, *J. Faculty of Eng. Univ. of Tokyo(B)*, Vol.40, pp.9-52, 1989.
14) Salem, H., and Maekawa, K., Spatially averaged tensile mechanics for cracked concrete and reinforcement under highly inelastic range, *J. Mater. Conc. Struct. Pavement*, JSCE, pp. 277-293, 1999.
15) An, X., Maekawa, K. and Okamura, H.: Numerical simulation of size effect in shear strength of RC beams, *J. Materials Conc. Struct., Pavements, JSCE*, Vol.35, No. 564, pp.297-316, 1997.
16) Mishima, T., and Maekawa, K.: Development of RC discrete crack model under reversed cyclic loads and verification of its applicable range, *Concrete library of JSCE*, No.20, 1992.

(Received April 18, 2000)

先行ひび割れを有するRC部材のせん断挙動に対する多方向固定ひび割れモデルの適用

ピマンマス　アモン・前川　宏一

先行ひび割れを有するRCはりのせん断破壊挙動を対象として,鉄筋コンクリートの力学における多方向固定ひび割れモデルの適用性と精度の検証を行った.数値解析において,1)多方向載荷と履歴依存性の考慮,2)多方向ひび割れを有するコンクリートの取り扱い,3)ひび割れ面におけるせん断伝達特性と異方性の表現が不可欠な問題であることが確認された.この要件に対して,独立非直交の4方向ひび割れモデルを適用することが可能なこと,また先行ひび割れを有するRC部材のせん断破壊等の解析結果と実験結果の比較から,このモデル化が十分有効であることを検証した.